LIMITATIONS ON WIND-TUNNEL PRESSURE SIGNATURE EXTRAPOLATION

Robert J. Mack
Langley Research Center
Hampton, VA

Christine M. Darden
Langley Research Center
Hampton, VA

SUMMARY

Analysis of some recent experimental sonic boom data has revived the hypothesis that there is a closeness limit to the near-field separation distance from which measured wind tunnel pressure signatures can be extrapolated to the ground as though generated by a supersonic-cruise aircraft. Geometric acoustic theory is used to derive an estimate of this distance and the sample data is used to provide a preliminary indication of practical separation distance values.

INTRODUCTION

Whitham's body of revolution flow field prediction theory, reference 1, and Walkden's extension to lifting wing-bodies, reference 2, have enabled engineers and designers to predict wind-tunnel flow-field pressure and ground-level pressure signature characteristics from research models and supersonic aircraft for the past thirty years. Initially, comparisons between wind-tunnel measured signatures and theoretically predicted signatures varied from good to poor. Good agreement between theory and measured data was found to depend on Mach number, configuration complexity, model attitude, and the ratio of measurement distance to model length. Corrections to effective length for angle of attack removed one major source of disagreement, and a linear-theory restriction on area-rule volume computations to Mach numbers less than about 3.0 took care of another. With the introduction of a modified linear theory wing analysis code, reference 3, the degree of good agreement improved even more due to the empirical technique used to account for nonlinear Mach number and wing thickness effects. Thus, it became possible to use the Mach-slice area-ruling feature of a wave drag code, reference 4, a modified linear theory lift analysis code, reference 3, and a corrected nacelle-wing interference lift code, reference 5, to calculate total equivalent areas from descriptions of wing, fuselage, nacelle, fin, and other components of complex wind-tunnel models and conceptual supersonic cruise aircraft. Then, good predictions of wind-tunnel and of ground-level pressure signatures were obtained using the Hayes' stratified-atmosphere propagation code, *ARAP*, reference 6.

A second method, reference 7, for obtaining ground-level signatures uses a pressure

signature measured near the wind tunnel model which is converted to an equivalent F-function. The Hayes' *ARAP* propagation code uses this F-function as an input, and predicts the ground-level overpressure signature.

A third method of obtaining ground-level signatures, presented by Thomas in reference 8, is a variation of the second method. A wind-tunnel pressure signature, measured under the model, is expressed in waveform parameters and then extrapolated through a stratified, standard atmosphere from a short distance under the aircraft at cruise altitude to the ground. This method also obviates the need for the detailed geometrical descriptions of the aircraft and for the analytical codes which calculate equivalent areas from volume and lift distributions. Since both the Thomas method and the Hayes' method assume that the disturbances are propagated in a two-dimensional manner, both give similar results.

A fourth method employs an Euler, a Full potential, a Parabolized Navier-Stokes, or some similar higher-order Computational Fluid Dynamics, *CFD*, code to calculate a pressure signature close to the model or aircraft. Then, as with the previous method, this signature is extrapolated to the ground through a stratified, standard atmosphere by the *ARAP* or the Thomas propagation codes.

With the design and construction of larger, more complex wind tunnel models to capture more aircraft details, and the increased use of *CFD* codes to predict near-field overpressures, a question surfaced concerning the minimum separation distance to insure that an extrapolated pressure signature would accurately represent a measured ground-level overpressure signature. It arose from numerical and computational requirements imposed by the development of these new *CFD* codes, from the size of these new, larger, more sophisticated wind tunnel models, and from the cross-section area of existing wind-tunnel test sections. The purpose of this paper is to explore the acoustical, mathematical, and aerodynamic nature of the problem to obtain a clear understanding of the situation, and to obtain some realistic boundaries and boundary parameters for workable answers to the problem. Wind-tunnel data will be used to support the hypothesis that limits are necessary, and as guidelines in support the analytic/empirical prediction of near-field limits on wind tunnel model-probe separation distances.

SYMBOLS

b	wing span, ft
CFD	Computer Fluid Dynamics
$F(x)$	Whitham F-function
h	distance in z-direction from wing apex or body nose to field line, in or ft
l	wing lifting length or root chord length, ft

M   Mach number

p   free-stream ambient pressure, psf

Δp increment in pressure due to model/aircraft flow field, psf

r   radius of the Mach cone touching the wing tip trailing edges with vertex along a line at distance h, ft

x   distance along the longitudinal axis, in or ft

x_1, x_2 distance, in x-direction, to the Mach cone vertices from the wing apex, ft

Δx difference in lengths, $x_2 - x_1$, ft

y   distance normal to the x-axis in the wing spanwise direction, ft

z   distance normal to the x-y plane, ft

α angle of attack, degrees

β Mach number parameter; $\sqrt{M^2 - 1.0}$

γ ratio of specific heats, 1.40 for air

η normal distance between the local span line and the Mach cone touching the wing tips (see figure 8), ft

μ Mach angle, $\sin^{-1}(1.0/M)$, deg

WIND TUNNEL MEASUREMENTS AND EXTRAPOLATIONS

An analysis of some recent experimental data demonstrated that the question of a minimum initial pressure measurement distance for the extrapolation of pressure signatures needed to be resolved. The experimental data were signatures measured from models designed to generate specially-shaped pressure disturbances meant to persist in form, but not strength, from cruise altitude to the ground. Figures 1 and 2 show samples of these wind-tunnel pressure signatures measured in test section one of the Langley Unitary Plan wind tunnel.
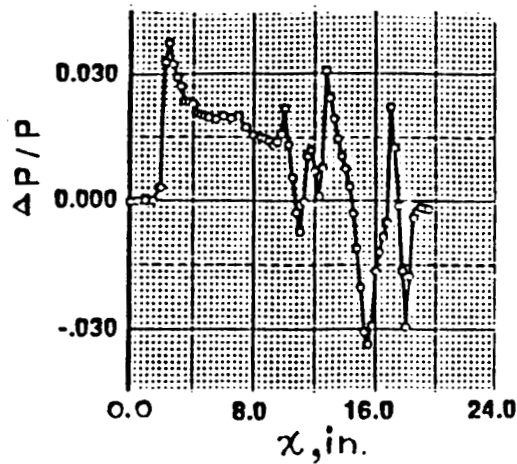
Figure 1. Pressure signature from the Mach 2.0 model at M = 2.0 and h = 6.0 inches

In figure 1, the signature was measured at six inches, (about 0.50 body length or about 0.94 span length), while in figure 2, it was measured at twelve inches (about 1.0 body length or about 1.88 span lengths).
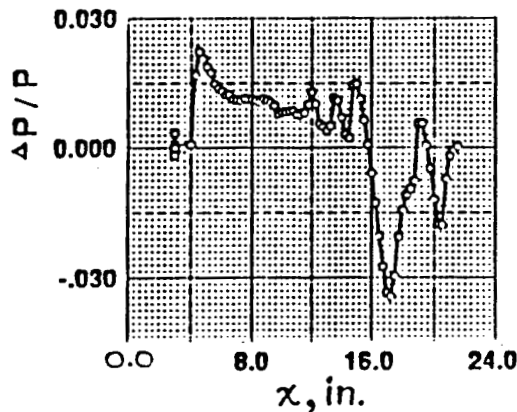

Figure 2. Pressure signature from the Mach 2.0 model at M = 2.0 and h = 12.0 inches

Test conditions for these signatures were a Mach number of 2.0 and a Reynolds number of 2.0 million per foot. The code developed by Thomas, reference 7, was used to predict the signature at twelve inches when extrapolated from one measured at a distance of six inches. In figure 3, the extrapolated signature and the measured signature at twelve inches are compared.
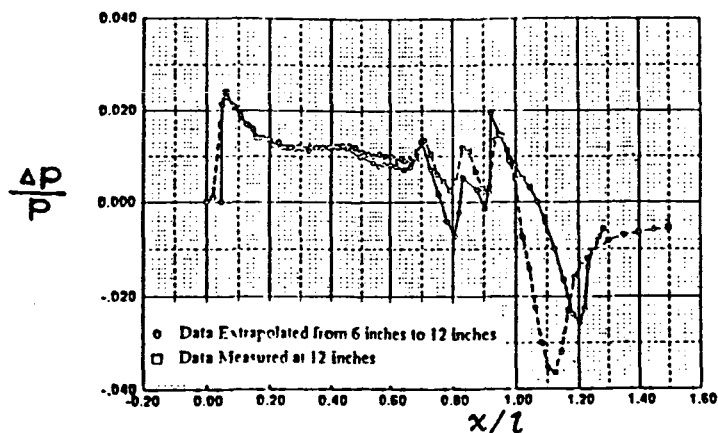
Figure 3. Comparison of the signature measured at twelve inches to the signature measured at six inches and extrapolated to twelve inches, M = 2.0 .

The two signatures agree very well near the nose. However, aft of $x / l = 0.4$, differences suggest that some of the three dimensional features of the flow field found at six inches have coalesced and merged. However, the extrapolated signature does not display this to the same degree as the measured signature. Next, the wind tunnel pressure signatures were treated as though they were measured at one-half and one body lengths below a full-sized aircraft and extrapolated from a cruise altitude of 55,000 feet to the ground, using the Thomas code. The signatures obtained are shown and compared in figure 4.
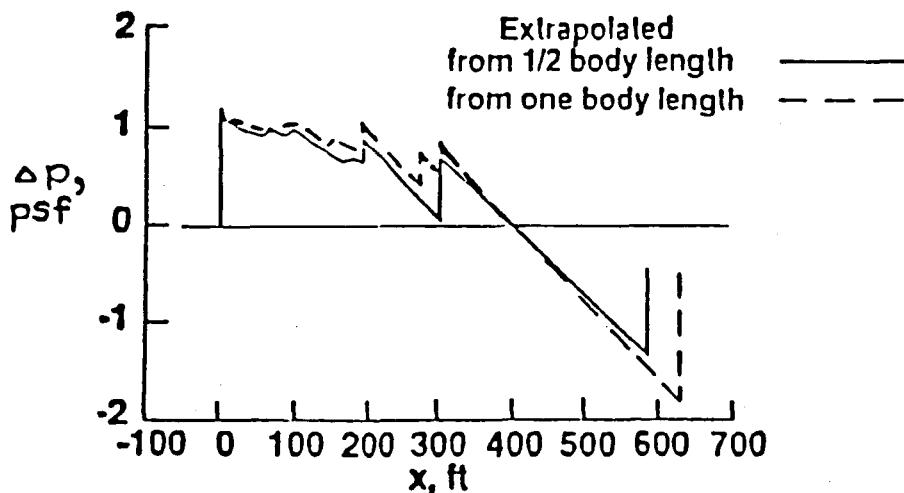

Figure 4. Comparison of pressure signatures measured at one-half and one body length, extrapolated from cruise altitude to the ground, M = 2.0 .

The two extrapolated pressure signatures show similar overall features. Again, there are differences that suggest that they came from aircraft with similar, though slightly different,

205

geometry. In figure 5, these extrapolated wind tunnel signatures are compared with a theoretical signature obtained from a sonic boom analysis of aircraft geometry which included only its fuselage-wing volume and lift contributions.
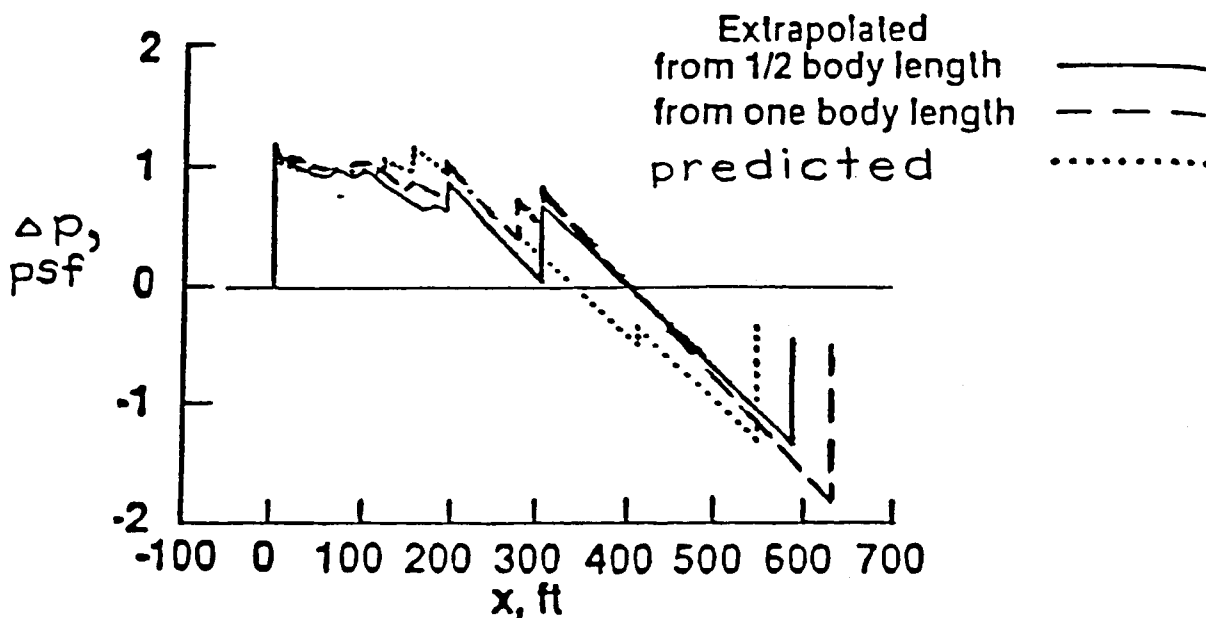

Figure 5. Comparison of extrapolated and predicted ground pressure signatures, M = 2.0 .

Three similar yet noticeably different signatures are seen. Since the same atmosphere was theoretically traversed by each pressure signature, the unique shape of each pressure signature suggests that perhaps different F-functions were calculated and extrapolated, or different pressure signatures were measured and extrapolated.

Since the F-functions were derived from measured pressure signatures, and the measurements were taken at two different separation distances, it would be logical to assume that the separation distance is a factor. Close in, three dimensional flow features permeate the shock and pressure field, while further away, some shock coalescence and flow smoothing has taken place. A further consideration arises from the shock waves of a sufficient strength, $\Delta p / p > 0.10$, (usually this ratio is less than about 0.02 on wind tunnel signatures) to be outside the theoretically small disturbance limitations of the prediction and propagation methods developed by Whitham and Hayes. This consideration would not apply in this case since the overpressures shown in figures 1, 2, and 3 do not exceed the aforementioned disturbance threshold.

Another factor to be considered in the analysis is the effect of Reynolds number. The wind tunnel tests were conducted at a unit Reynolds number of 2.0 million per foot. At a cruise altitude and a cruise Mach number of 55,000 feet and Mach 2.0 , the unit Reynolds number is about 1.87 million per foot, a difference in unit Reynolds number which is relatively small. However, the scale factor between the model and the aircraft is 1.0 : 300.0 . So the displacement thickness and volume

on the model is disproportionately large compared with that on the full-scale aircraft. Any extrapolation of extreme near-field wind tunnel overpressure signatures to obtain ground pressure signatures will carry these scale effects as well as fuselage/wing-lift three-dimensional effects and exaggerate their influence. However, extrapolation of wind tunnel pressure signatures can be done after the signatures which have been measured at reasonable distances have been corrected to full-scale Reynolds number conditions, a commom treatment for force-model data.

A final point to be considered concerns the engine nacelles even though they were not on the models whose signatures are shown in figures 1 to 5. These components are very small because the aircraft model is small. Even the largest sonic boom models are only about twelve inches in length and six inches in span. Their finite-strength shock waves in the extreme near field come directly from the inlet lip and from shock wave reflections off of the lower surface of the wing. They are discrete-disturbance bodies in the flow field of the wing-fuselage which have tailored, blended, and distributed-disturbance surfaces. Since they are usually well aft on the aircraft, their pressure disturbances are closer to the measurement probe than the nose and forebody because of wing-fuselage camber and model angle of attack. In the extreme near field, they generate prominent, superimposed waves; in the mid-field and cruise distance-field, their shock waves attenuate rapidly and blend gradually into a quasi-two dimensional wave pattern. While the nacelles are important, the wing lift will be the primary subject of this paper because it is the dominant source of pressure disturbances from the aircraft. However, some comments on the magnitude and effect of the disturbances produced by the nacelles will be forthcoming later.

THEORY

Whitham's body-of-revolution theory, and Walkden's extension of this theory to wings at lifting conditions, were the basis of a method for predicting the disturbance felt on the ground from the flow field disturbances of an aircraft cruising at supersonic speed. The method was based on a thin, slender aircraft, small induced shock and pressure disturbances, low to middle supersonic range Mach numbers where real gas effects are negligible, and the observer being far from the flight path. This last condition assures that the pressure disturbances perceived by a ground observer were propagating in a two-dimensional manner through the atmosphere.

Although these conditions are met with an aircraft at cruise altitude with the observer on the ground, not all are met when a static pressure probe is in close proximity to a wind-tunnel model. If the model is a slender body of revolution aligned with the flow, these condition are met at very close distances because the body diameter is small relative to the measurement separation distance, the pressure disturbances are small compared with the ambient pressures, and the body is not developing lift. It is the presence of lift as well as volume on a wing-body model that causes three-dimensional, near-field flow features such as vortex flow, local separation and reattachment, boundary layer transition, etc. that are not handled accurately by the two dimensional extrapolation

methods when applied to data measured in the extreme near-field.

The cylindrical propagation model presumes that all disturbances are about equally distant from the observer. With the observer in close and the aircraft or model at finite angle of attack, the disturbances from the aft end are disproportionately represented. At a mid-field rather that a near-field distance, these three-dimensional characteristics of the flow field blend and merge so that the characteristics of the real propagation field more closely agree with those of the theoretical propagation model. This limitation is accounted for in sonic boom analysis using the ARAP code, where the initial signal at three body lengths assumes a cylindrical mode of propagation.

Extreme near-field pressure measurements can also produce a second source of error. Pressure disturbances from model or aircraft volume and lift effects that are felt at a point in the flow field are bound within a limiting characteristic surface usually represented by a Mach cone. With the observer on the ground, this cone extends so far that the section of its surface that intercepts the aircraft is essentially flat. Thus, far-field Mach slicing planes can be used in the analysis of cruise aircraft sonic boom characteristics. The wind-tunnel conditions, on the other hand, are near-field, depending on model size, so the Mach-cone surfaces "passed" through the model to obtain a distribution of the disturbance sources are very curved. Figure 6, a two-view of a slender aircraft in supersonic-cruise flight can be used to illustrate these ideas.
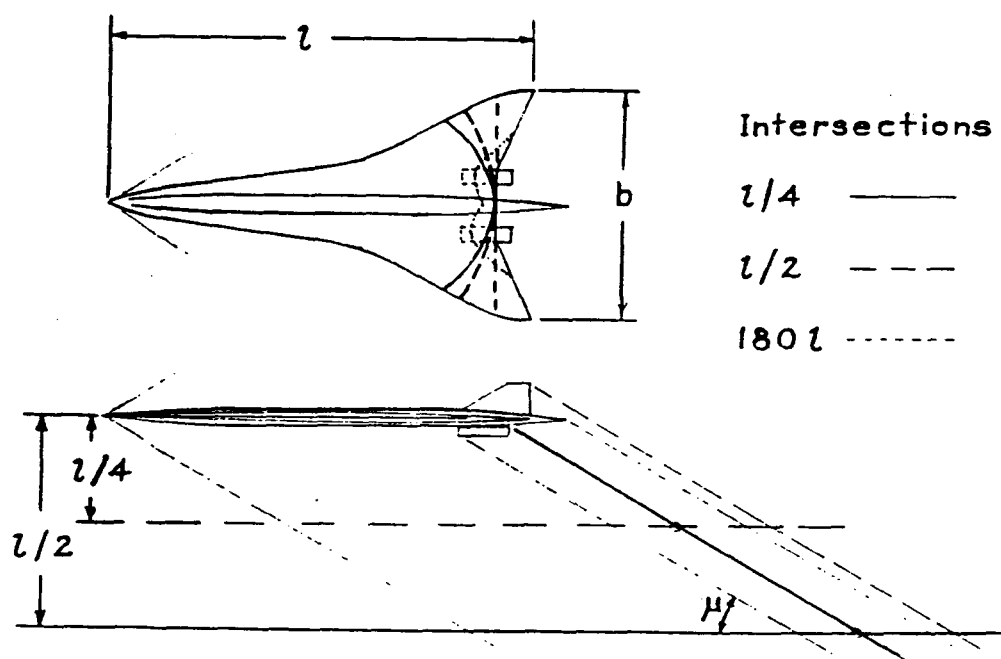

Figure 6. Two-view of aircraft in supersonic cruise flight.

Observers or probes beneath the aircraft and along a Mach line from the wing trailing edge will see disturbances forward of the indicated Mach cone-wing intersection curves; Mach cones whose vertices are at the three indicated distances and on the Mach line. The additional disturbance

sources that are felt as the observer moves further away will show in the character of the calculated F-function or on the measured pressure signature. This is especially important since the aircraft designer with low sonic boom constraints is using the ground reference plane which is about 180.0 body lengths distant. In contrast, wind tunnel measurements are taken at separation distances of one-half to three or so body lengths. So, a Whitham F-function derived from these near-field, Mach-cone intercepted areas will not be the same as a Whitham F-function calculated from planar, far-field, Mach-plane intercepted areas, will not give the same signatures, and will not conform to the framework of Whitham's method except in an approximate way. A simple example will illustrate this point. It will also serve as a basis for establishing limits on the near-field distance used to obtain overpressure signatures that can be reliably extrapolated from cruise altitude to the ground.

The lift from an extended wing surface is the dominant disturbance contribution on an aircraft or a wind-tunnel model of a supersonic cruise aircraft. At cruise conditions, the equivalent area due to lift can be eight to ten times larger than the equivalent area due to volume at the aft end of the aircraft. To focus on the area-rule treatment of the lift distribution in this analysis, a conceptual low-boom configuration at cruise conditions has deliberately been simplified to a thin, uncambered wing with zero dihedral. Camber, twist, dihedral, and airfoil thickness would add realism, but not clarity, to the picture and have been omitted. The wing at a low angle of attack is shown in figure 7 along with some near-field wave characteristics.
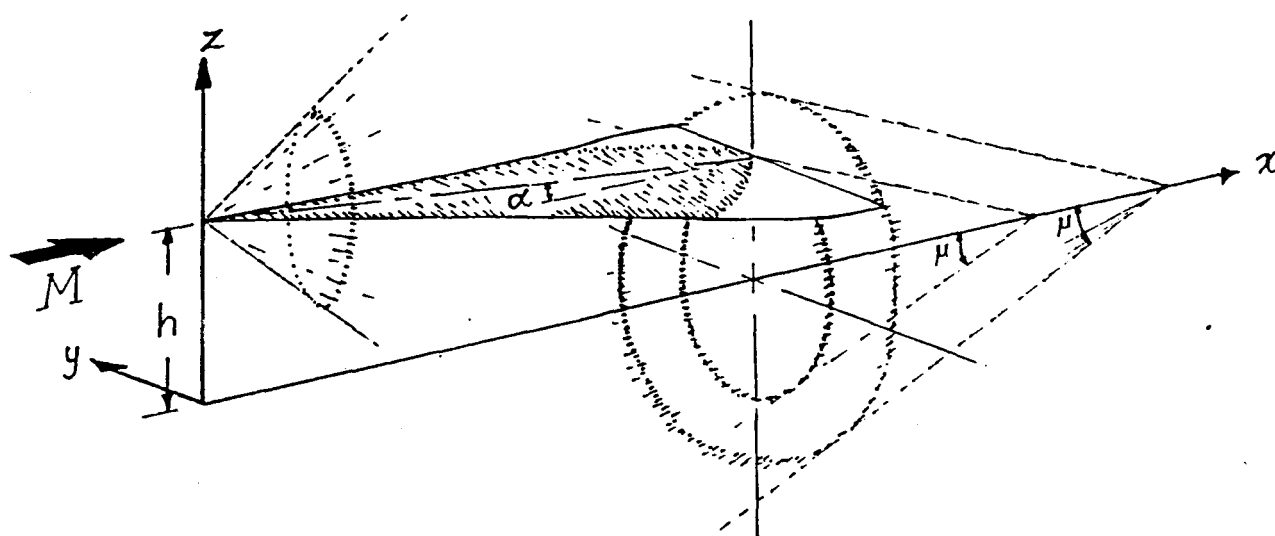

Figure 7. Slender wing at angle of attack in supersonic flow.

The simplified wing has all the essentials for examining the treatment of the lift distribution because it now depends only on planform shape. The flow field characteristics which focus at the

vertices have complex curvature due to local pressure perturbations. However, to keep the analysis simple, these characteristic surfaces will be assumed to have the shape of Mach cones. Note that the Mach cone that intersects the wing root chord trailing edge intercepts only part of the total lifting pressures. When this Mach cone moves a short distance aft, it touches both tips and encompasses all the lifting pressures. Now note, as was mentioned in figure 6, that a Mach cone with its vertex at a hundred or more span lengths away intercepts all the lift as it lays tangent with the first Mach cone position. In what follows, the ramifications of these observations will be explored. A three view drawing of this sketch, figure 8, is presented so that the methods used in the analysis of the longitudinal lift distribution can be easily explained.

Figure 8. Three view of lifting wing in supersonic flow.

The front view shows the intersection of the wing-tip Mach cone, vertex at x_2, with a plane normal to the x-axis which touches the trailing edge of the wing tips. A projection of this Mach cone into the x-y plane, including the lines through vertex point x_2, is seen in the top view.

The side view shows the wing-tip Mach cone projection onto the x-z plane intersecting the x-axis at x_2, the wing root chord, and a Mach line from the wing's root chord trailing edge to the point x_1 where it crosses a line parallel to the flow velocity vector at a measurement distance, h. Wing geometry and acoustic characteristic lines shown in this three view are used to describe the flow field characteristics felt by an observer in the near- and far-field.

Since each view is a projection onto a plane, the Mach cones appear as lines. This simplifies the discussion of both near-field and far-field characteristics. In the far-field, the curvature of the Mach-cone surface passing through the wing is almost infinite i.e. the surfaces used to "slice" the wing are nearly planar. In the near-field, the important intersections of the Mach cone with the wing are well defined. The distinctive features of both the near-field and the far-field are used to determine a reasonable distance at which theoretical or experimental signatures can be extrapolated with accuracy and confidence from under the aircraft to the ground.

A Mach cone with its vertex at x_1 intercepts the wing at the trailing edge of the root chord; at points on the wing ahead of the trailing edge, the intersection of the Mach cone and the wing surface is a conic curve. Thus, some of the wing's outer volume and lift-disturbance sources are not felt at x_1 as seen in figure 8. However, the Mach cone that just touches the wing tip trailing edges, where the lift growth has reached its maximum level, has its vertex at x_2. Using acoustic theory to keep the mathematics and physics simple, the longitudinal distances to these field point locations noted in figure 8 are:

$$x_1 = l\cos\alpha + \beta (h - l\sin\alpha) \tag{1}$$

and

$$x_2 = l\cos\alpha + \beta r \tag{2}$$

there

$$r^2 = (b/2)^2 + ((h - l\sin\alpha)^2) \tag{3}$$

Clearly, x_2 is greater than x_1 ; the difference depending on the Mach number, the angle of attack, the distance, and the wing span. At the distance, h , from the model/aircraft, the incremental length, Δx , which is the distance between the the vertex of the Mach-cone touching the tips and the Mach-plane touching the root chord trailing edge can be represented by the equation

$$\Delta x = x_2 - x_1 = \beta (r - h + l\sin\alpha) \tag{4}$$

While this distance increment could be used to measure the differences between near-field and far-field wave characteristics, a more reasonable measure of the local Mach cone curvature can be estimated from η , the normal distance from the local span line to the Mach cone

$$\eta = \Delta x\ \sin\mu = \Delta x/M = \frac{\beta}{M} (r - h + l\sin\alpha) \tag{5}$$

If the separation, h , is sufficiently large, this distance should be small relative to the wing span, b , the wing chord, 1 , or the wing root chord projection, 1 cos α . Along the observational line at separation distance, h , and parallel to the x-axis, both the mid-field and the far-field F. functions would be similar and resemble the measured disturbance if it were further away than some limiting distance which will be derived in the Discussion. Beyond this limiting separation distance, an extrapolation of the near-field F-function or its counterpart derived from a near-field pressure signature using

$$F(x) = \frac{\sqrt{2.0\beta h}}{\gamma M^2} / \left(\frac{\Delta p}{p}\right)$$

(6)

taken from reference 1, would provide a reasonably accurate estimate of ground overpressures or the corresponding noise loudness. Although this discussion and the derived equations are somewhat simplified, they are based on experimental data, figures 1 and 2, and highlight the need for measuring data at separation distances which are consistant with the limitations of the applicable propagation theory.

Whitham derived the F-function and the corresponding characteristic equation on the basis of far-field assumptions. Experience has demonstrated that both can be used in the mid-field and in some near-field situations if certain slenderness conditions are met. Using equation (5) to determine criteria for minimum measurement distances is very empirical since it is derived from geometrical acoustics. A wing having camber, twist, dihedral, and a trailing edge with forward or rearward swept sections would not fit neatly into this model framework. However, at distances along the root chord and forward of the trailing edge, local span lines would approximate a wing section where equation (5) would apply if the wing camber and twist were not severe. The aeroacoustic modeling of the wing and the Mach ray paths aft of this point would be more complicated, but would not refute the physical situation described by equation (5). Further, the measured extrapolated, and predicted pressure signatures presented in the *Wind Tunnel Measurements And Extrapolations* section, figures 1 to 5, show that most of the contributing flow field features associated with lift have already been identified. Thus equation (5) is useful because its derivation is straightforward and because it can be applied almost anywhere if the model or aircraft is as slender as required by high aerodynamic efficiency and low sonic boom requirements. In the *Discussion* section which follows, these equations and ideas will be developed further.

DISCUSSION

The need for determining proper near-field measurement distances so that wind-tunnel or theoretical pressure signatures can be extrapolated has been outlined and demonstrated in the

previous sections. There is no doubt that the extrapolation method is useful when a complete description of the model is unavailable, the machining inaccuracies are difficult to account for, or the model/aircraft scale factor is large (as it usually is with sonic boom models). The question is, as it was stated earlier: How small can model-probe separation distances be to insure that the measured pressure signatures are mostly two-dimensional in nature so as to maintain the extrapolation methodology from model/aircraft to the field-point/ground observer?

Begin the answer with equation (5) from the previous section. Substituting equation (3) into equation (5) and nondimensionalizing with b, the span, gives

$$\eta/b = \frac{\beta}{Mb} \ [\sqrt{0.25b^2 + (h - l\sin\alpha)^2} - (h - l\sin\alpha) \ ] \tag{7}$$

This can be simplified by assuming that, at typical aircraft attitudes,

$$h \gg l\sin\alpha$$

which is not an unusual flight or test condition. Using a binomial expansion, equation (7) can be simplified and expressed as

$$\eta/b = \frac{\beta}{M}/(8.0 \ h/b) \tag{8a}$$

or

$$\eta/l = \frac{\beta}{M} b^2/ (8.0hl) \tag{8b}$$

which indicates that it is span rather than length which is of first-order importance.

To judge how well equation (8a) approximates equation (7), a comparison of η/b values calculated from equation (7) and (8a) are shown in figure 9 for $M = 1.6$, $l = 300.0$ feet, $b = 160.0$ feet, and $\alpha = 2.0$ degrees.
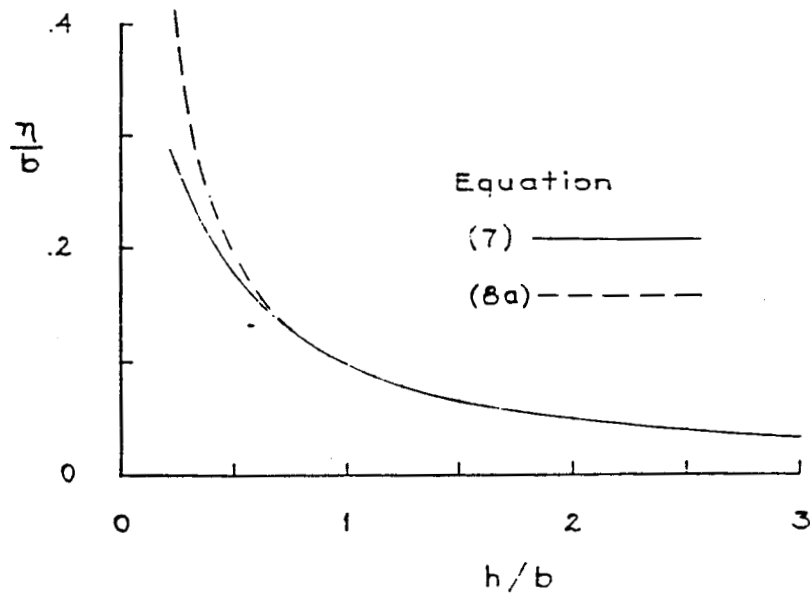
Figure 9. Comparison of η/b values from equations (7) and (8a), $M = 1.6$.

The Mach number in equations (7) and (8a) is seen to be a strong influence on the value of η/b, but the values obtained from the two equations disappear after a separation distance of about 0.75 span lengths. A comparison of η/b values calculated from equation (7) for three cruise Mach numbers are shown in figure 10 for the sample conceptual aircraft with $l = 300.0$ feet, $b = 160.0$ feet, and $\alpha = 2.0$ degrees.
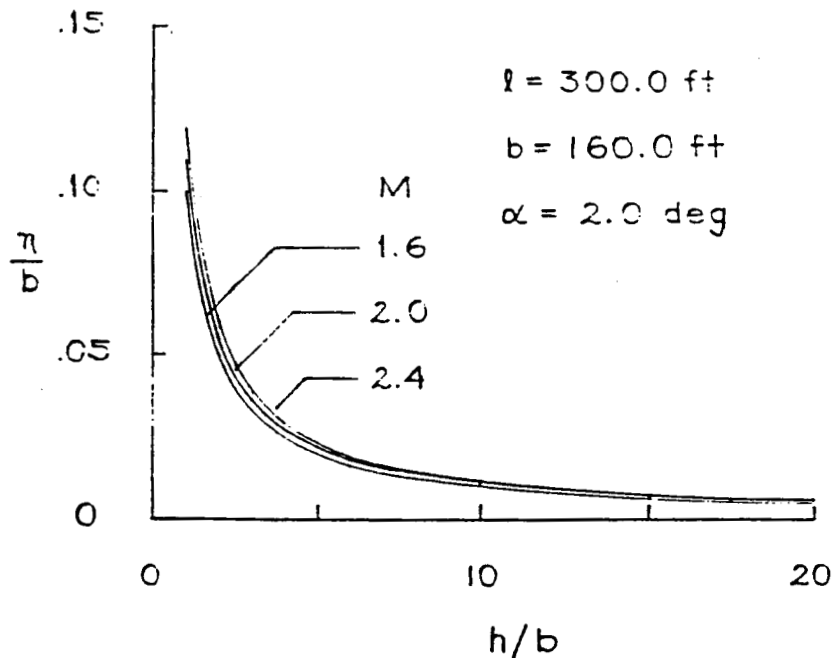

Figure 10. Comparison of results from equation (7) for Mach numbers of 1.6, 2.0, and 2.4.

214

At increasing Mach numbers, the condition that η/b be small will be increasingly more difficult to meet for a distance, h , found in wind tunnel test sections which will be between one and ten span lengths (about one-half and five body lengths). Aircraft length is seemingly unimportant but enters implicitly through the high-aerodynamic-efficiency-cruise condition that the span/length ratio, b/l , be small; usually it is about 0.50 or less.

Since aircraft length, l , can be replaced by the more general length, x , when the span is interpreted as the local span, b(x) , equation (8) permits local span conditions to be readily calculated and some conclusions to be made. Figure 11 shows the change in η/b along the longitudinal length of a delta wing when l = 300.0 feet, h = 150.0 feet, b =160.0 feet, M =2.0, and α = 2.0 degrees. For comparison, the values of η/b on an uncambered Mach 2.0 wing are also shown. Note that in this example, h / l is 0.5, a typical near-field condition.
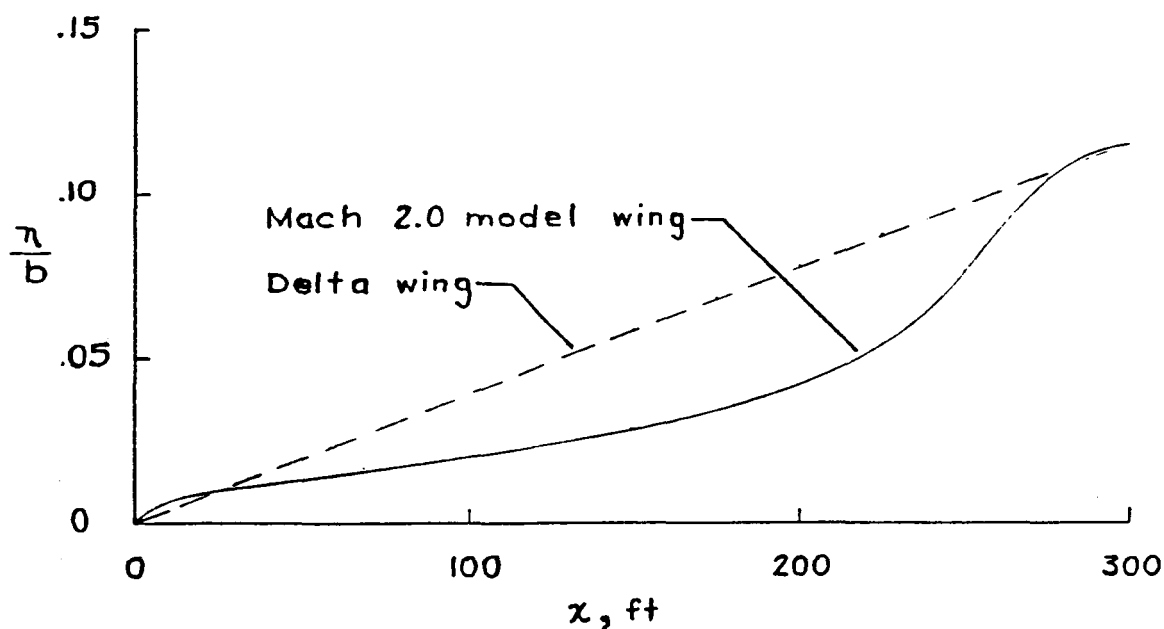

Figure 11. Variation of η/b along a delta wing and a flat Mach 2.0 model wing.

It should be noted that the delta wing will have more area than the Mach 2.0 wing and will therefore generate more lift at the given angle of attack, α , of two degrees. However, the differences between extreme near-field and far-field conditions under discussion are based on wing geometry rather than lift.

The desired condition that η/b or η/l be small is usually met at the nose of the aircraft because the local span is much less than the full span. Moving rearward along the aircraft, the local span increases reducing the value of the ratio, b/h , and increasing the magnitude of η/b , an effect more noticeable on the delta than on the Mach 2.0 aircraft wing. Predictions of overpressures near the nose from far-field codes would be in good agreement with measurements because the

215

corresponding part of the F-function would be appropriately mid- to far-field. As the wing leading edge sweep decreases, the rapid build-up in span and lift alters the nature of the F-function intended for extrapolation. The F-function changes, as the length increases, from one that is mid- to far-field, to one which is more near-field, providing an extrapolation F-function which would push the limits of propagation theory accuracy.

These results have provided information and a method to answer the questions. How small a separation distance is permitted to assure accurate and reliable extrapolations from cruise altitude to the ground? One possible level of certainty could be obtained from selecting a "curvature" limit, η/b, such as

$$\eta/b = 0.01$$

which gives, using equation (8a)

$$h/b = 12.5 \, \frac{\beta}{M}$$

or from equation (8b)

$$h/l = 12.5 \, \frac{\beta}{M} \, b/l$$

Applying this to a body of revolution at zero angle of attack such as a 4.0 degree semi-vertex angle cone in Mach 2.0 flow, the span, b, would be replaced by the maximum cone diameter. Using h/l as a parameter because the cone has no "span" leads to the value

$$h/l = 1.514$$

For the aircraft with dimensions given in figures 9, 10, and 11, the value of h/l obtained is

$$h/l = 5.774$$

This one-percent-of-span limit is very restrictive and may be a more demanding limit than can be met in most supersonic flow test sections. However, it does provide a reasonably conservative value of a limiting distance.

A second possible level would be a more lenient value of η/b such as

$$\Delta x/b = 0.05$$

which results in

$$h/b = 2.5\frac{\beta}{M}$$

or

216

$$h/l = 2.5 \ \frac{\beta}{M} \ b/l$$

For the four-degree semi-vertex angle, slender cone example, this results in

$$h/l = .303$$

while for the sample aircraft dimensions

$$h/l = 1.154$$

The five-percent-of-span requirement is much less demanding and is within the measurement limits of the larger supersonic wind tunnel test sections. An in-between value of

$$\eta/b = 0.025$$

would insure that the desired propagation characteristics would be adequately maintained while allowing latitude for test section and *CFD* code limitations. This value, using dimensions from the example aircraft at $M = 2.0$, gives

$$h/l = 2.309$$

a value which can be met in many of the larger supersonic-flow wind tunnel test sections.

These are arbitrarily selected values which were used because of the sparsity of experimental data. If the available data, figure 5, is pressed into service, some very tentative indications can be found. In figure 5, the values of h/l for each signature are 0.5, 1.0, and 171.9, with the corresponding values of η/b being 0.1187, 0.0596, and 0.0003 respectively. The agreement between the signatures is good only for about the first one hundred feet. The value of η/b which corresponds to this length (see figure 11) is about 0.016 to 0.020, not a strong recommendation for extrapolations of pressure signature measured at one or less body lengths. However, much more data is needed to verify such a call for separation distances of three and more body lengths (six and more span lengths).

This method was derived from simplified geometrical acoustics and therefore is empirical in its form as well as conservative in its predictions. Very likely, a more exact, higher-order method which accounted for flow-field disturbance strengths would yield similar but even more restrictive

predictions. This higher-order method would use multiply-curved characteristics surfaces which would trace the propagation paths originating from the compression and expansion regions. No matter what separation distance is chosen for the measurement of pressure data, this method can provide, using equation (7) or (8a), a numerical evaluation of how closely the wind tunnel data is approximating a two-dimensional propagation wave-form and how credible an extrapolated ground-level pressure signature can be expected.

COMMENTS AND QUALIFICATIONS

The Whitham F-function has been refered to several times in this report because it acts as the disturbance potential of an equivalent body of revolution which represents a real body of revolution, a wing, or even an aircraft in supersonic flight. This F-function can be calculated if a full description of the geometry is available, and if an accurate lift distribution can be estimated from the geometry should the wing-body be at a lifting attitude. It can also be derived from a pressure signature measured at a separation distance where three dimensional flow features have, for the most part, settled out. Flow field disturbances at various distances can then be predicted from this F-function in the various wave propagation theory, altitude, and atmosphere models. The key point in this discussion is that the same F-function be used throughout the flow field between the aircraft and the ground to obtain predicted pressure signatures.

It is with these theoretical and experimental limitations as a base that equations (7) and (8) were derived. Obviously, the value given to η/b or η/l can be relaxed further than those mentioned, but these larger values and corresponding less-accurate representations of the mid-field or far-field ground observer's F-function introduce an increasing loss of accuracy.

A similar discussion could be directed toward the area-rule treatment of the interference-lift produced on the wing lower surface by engine nacelles. Without going into more details than have been presented, the nacelles generate discrete pressure disturbances which will require a different limiting distance before they blend into the established wing-fuselage pressure signature pattern desired by the aircraft designer. The shock waves generated and their reflections off the wing lower surface will merge and coalesce only after spreading outward for several span lengths. Thus, the distances suggested in this paper are conservative near-field estimates and measurements at distances farther away are definitely desireable.

Reynolds number effects will have to be treated in a manner similar to that used to correct wind tunnel drag data. The CFD code that best predicts the pressure signatures at the wind tunnel Reynolds number will be used to predict the pressure signature at free flight Reynolds number at a suitable separation distance. This pressure signature could then be extrapolated to obtain a ground signature which would be representative of those generated by the real aircraft in supersonic cruise mode.

CONCLUDING REMARKS

A need to determine limits on near-field separation distances at which experimental pressure signatures will be measured for the purpose of extrapolation from aircraft to the ground has been discussed and established. Empirical means for estimating these limits were derived from simple models and first-order acoustic theory and were shown to depend primarily on the local or total wing span, b, the distance from the wing or model/aircraft nose to the field line, h, and the Mach number through the parameter, β. A second-order dependence on the wing length, l, and the effective angle of attack, α, was shown to be of lesser effect except at extreme near-field distances in very close proximity to the wing or lower body surface.

The results of this study cast some doubt on the accuracy of ground-level signatures obtained by extrapolating experimental signatures measured at 1.0 or less span lengths, h/b, from the model/aircraft. Limits obtained in the discussion indicated that one to two body lengths for a slender body of revolution and from 9.0 to 13.0 span lengths, depending on Mach number, are needed to permit the three-dimensional aspects of the Mach-cutting surfaces sufficient distance to decrease in curvature so that the equivalent area growth stays within the limitations of two-dimensional propagation characteristics. These separation distances were obtained from arbitrary and conservative limits on the "curvature" parameter η/b. It was also shown in the discussion that more lenient values of this parameter might permit usable signatures as close as 4.0 to 5.0 span lengths (about 2.0 to 2.5 body lengths) depending on Mach number. However, the brief discussion of nacelle integration effects on near-field pressure measurements added emphasis to the recomendation that measurement distances should be as large as is practical for a given wind tunnel test section cross section.

REFERENCES

1. Whitham, G. B. : The Flow Pattern of a Supersonic Projectile. Comm. Pure & Appl. Math., vol. V, no. 3, Aug. 1952, pp. 301-348.

2. Walkden, F. : The Shock Pattern of a Wing-Body Combination, Far From The Flight Path. Aeronautical Quarterly, vol. IX, pt. 2, May 1958, pp. 164-194.

3. Carlson, Harry W. and Mack, Robert J. : Estimation of Wing Nonlinear Aerodynamic Characterisrics at Supersonic Speeds. NASA T. P. 1718, 1980.

4. Harris, Roy V. , Jr. : A Numerical Technique for Analysis of Wave Drag at Lifting Conditions. NASA TN D-3586, 1966.

5. Mack, Robert J. : A Numerical Method for Evaluation and Utilization of Supersonic Nacelle-Wing Interference. NASA TN D-5057, 1969.

6.   Hayes, Wallace D., Haefeli, Rudolph C., and Kulsrud, H. E.: Sonic Boom Propagation In A Stratified Atmosphere, With Computer Program. NASA CR-1299, 1969.

7.   Hicks, Raymond H. and Mendoza, Joel P. : Prediction of Aircraft Sonic Boom Characteristics From Experimental Near Field Results. NASA TM X-1477, 1967.

8.   Thomas, Charles L. : Extrapolation of Sonic Boom Pressure Signatures by the Waveform Parameter Method. NASA TN D-6832, 1972.